Master's Thesis of Landscape Architecture

Multi-objective Optimization Model for 3D Urban Green Space to Reduce Urban Heat Island

도시열섬 저감을 위한 3차원 도시 녹색 공간에 대한 다목적 최적화 모델

August 2022

Graduate School of College of Agriculture and Life Sciences
Seoul National University
Landscape Architecture Major

Zhenggang Piao

Multi-objective Optimization Model for 3D Urban Green Space to Reduce Urban Heat Island

Under the Direction of Adviser, Prof. Dong Kun Lee

Submitting a master's thesis of Public Administration

August 2022

Graduate School of Agriculture and Life Sciences
Seoul National University
Landscape Architecture Major

Zhenggang Piao

Confirming the master's thesis written by Zhenggang Piao
August 2022

Chair Heeyeun Yoon
Vice Chair Junsuk Kang
Examiner Dong Kun Lee

Abstract

With rapid urbanization, the type of land cover and spatial composition of cities have changed dramatically. These changes have had significant impacts on the urban environment, such as the urban heat island (UHI) effect. UHI has a significant impact on greenhouse gas emissions, energy consumption, and the health of residents.

Urban Green Spaces (UGS) are an effective way to address the urban heat island effect. UGS can reduce temperatures by providing shade and evapotranspiration. There are several types of UGS, with the most popular methods currently being green roofs, green walls and street trees. They can be effective in providing heat reduction benefits to cities without taking up too much space for urban development.

The location, type, size and number of UGS have a significant impact on their thermal effect. With limited construction cost of urban green space, the selection of green space and the right size of installation area are key factors to achieve high cooling efficiency.

However, in previous studies, UGS planning was carried out using 2D methods, which are unable to evaluate wall greenery and mainly use statistical methods to evaluate the cooling effect of greenery due to the limitations of 2D. In this study, we intend to build a 3D Multi-objective Optimization Model to optimize the layout of green spaces in the city. The spatial optimization algorithm NSGA II evaluates the trade-off between cost and cooling effectiveness by considering various parameters of UGS (type, size, location, cost, etc.) and derives the solution set of the optimal layout solution. The model is expected to provide urban planners with accurate and rational construction planning.

Keyword : Green infrastructure, Urban heat island, Spatial optimization, NSGA II, Cooling effect

Student Number : 2020-29420

Table of Contents

List of Figures

List of Tables

Chapter 1. Introduction

1.1. Study Background

With the rapid development of urbanization, the types of urban land cover and spatial configuration have undergone this tremendous change(Sun, Anchang, 2016). Such changes have a huge impact on the urban environment, such as the urban heat island(UHI) effect(Debbage, Nei, 2015). UHI has a huge impact on greenhouse gas emissions, energy consumption, and residents' health.

Urban Green Space(UGS) is one of the effective solutions to the urban heat island effect(Oliveira, Sandra, 2011; Getter, Kristin L, 2006; Ng, Edward, 2012; Bowler, Diana E, 2010; Cai Jing, 2011).UGS reduce the temperature by providing shade and evapotranspiration(Cai Jing, 2011; Liu, Jie, 2021). The shading effect in the UGS comes from the blocking effect of the plant canopy on radiation. Through this blocking, the radiation received by the surface can be reduced, thereby lowering the surface temperature(Winston TL Chow, 2016). The evapotranspiration of the UGS comes from the evaporation of water on the surface of the plants. The evaporation of water reduces the temperature of the air, thereby reducing the temperature of the UGS and its surroundings(Dimoudi, A, 2003). Due to the large number of plants in the green space, the albedo of the area can be changed to improve the radiation environment in the surrounding area, thereby reducing the surrounding temperature. (Taha, H, 1997).

As people pay more and more attention to urban heat islands, many cities are constantly trying to establish UGS to cope with climate change. There are many types of UGS, and so far, the most valued are roof greening, wall greening and trees. They can effectively bring heat reduction benefits to the city without occupying too much urban development space(MA Polo-Labarrios, 2020; O Addo-Bankas, 2021; I Bajsanski, 2019).

Although more than 90% of the UGS in a city brings about heat reduction, there are large differences in the heat reduction benefits depending on the location, type, size and number of UGSs (Arpit Shah, 2012). For example, larger walls Greening can provide higher cooling efficiency and larger radiation range (Hongyu Du, 2017). Even the same area of greening on the wall will have very different cooling benefits depending on the orientation of the wall where it is located. At the construction site of UGS, different cooling benefits will be produced due to the different material types of the original wall or floor. Furthermore, most UGSs provide better benefits in non-shaded areas than in shaded areas. Therefore, under the circumstance that the construction cost of urban green space is limited, the selection of green space types and the rationality of the setting area are the key factors to achieve higher cooling efficiency.

In order to find out how to better build UGS in urban areas, Yujia Zhang et al. developed a green space optimization model to evaluate the cooling trade-off between day and night. The results show that adding 1% of new green space will cause the surface temperature to decrease by 1–2 °C(Yujia Zhang, 2017). E.J. Yoon et al. tried to use the greening effect, construction cost and connectivity as the goal to establish an urban greening space planning model. The results showed that there is a synergistic relationship between greening effect and connectivity, and there is a trade-off relationship between greening effect and construction cost(E.J. Yoon, 2019).

However, in previous studies, UGS planning was performed with a 2D approach. Therefore, such methods cannot evaluate wall greening, and due to the limitation of 2D, statistical methods are mostly used in the evaluation of heat reduction benefits. Therefore, this study attempts to establish a 3D optimization model for the optimal arrangement of UGS. Based on various variables of UGS (type, size, location, cost, etc.), the cooling effect and neighborhood cooling are evaluated. The space optimization algorithm (NSGA2) is used to consider the trade-off relationship between cost and heat reduction benefit, and derive the optimal arrangement planning. It is expected that the model will provide urban planners with more accurate and reasonable construction plans.

1.2. Literature review

1.2.1 Impact on urban green space to mitigate UHI

The temperature in the center of the city is higher than that in the surrounding suburbs and rural areas. This phenomenon is called the Urban Heat Island effectUHI)(Peng, Shushi, 2012; TR Oke, 1988; Eugenia Kalnay, 2003; Fumiaki Fujibe, 2008). With the acceleration of urbanization, the impact of UHI on people is gradually expanding. The reasons for the urban heat island effect are as follows: (1) The construction of a large number of impervious layers in the city has led to a rapid change in the radiation environment, which has led to a rise in temperature. (2) The emission of artificial heat caused by high population density and urbanized lifestyle in cities has led to an increase in urban problems. Due to the increase in urban temperature caused by UHI, urban energy consumption has increased, urban air and water quality has deteriorated, and even the health of urban residents has been endangered McCarthy, Mark P, 2010; Santamouris, M, 2014; Tan, Jianguo, 2010).

Urban green space is one of the advantages to alleviate UHI. The UGS's mitigation mechanisms for UHI mainly include: (1) USG can change the albedo within the area, thereby changing the radiation environment, and then reducing the surrounding temperature Winston TL Chow, 2016; Su Li Heng, 2019). (2) The construction of UGS will increase the coverage of plants in the area. Therefore, the plant canopy will resist a large amount of radiation from entering the ground, thereby reducing the temperature of the ground Dimoudi, A, 2003; Taha, H, 1997). (3) Plants will not only provide a lot of shade, but also can pass evaporation of water on the surface of plant leaves provides evapotranspiration. Through evapotranspiration, heat energy can be converted into molecular energy, which in turn changes the temperature of the surrounding environment. The UGS not only acts on its internal space, but also has a cooling effect on the external space around the UGS through air circulation and heat exchange Francesc Baró, 2014; F Liu, 2021).

Therefore, the cooling effect of UGS is usually divided into two categories for evaluation. (1) Direct cooling benefit. Provides direct heat reduction benefits to walls or floors in the UGS setting area by blocking solar shortwave radiation. (2) Indirect cooling benefit. Provides heat-reducing benefits to the surrounding environment by reflecting less short-wave solar radiation, or by emitting less long-wave radiation by maintaining lower temperatures through evapotranspiration.

Based on the local situation in Seoul, South Korea, a combined analysis is carried out. Since most of Seoul has completed a high degree of urbanization development, and the urban characteristics of Seoul determine the high price of local land. Therefore, compared to building urban parks, setting green roofs, green walls and trees is a more suitable and economical choice. Therefore, this study will focus on green roofs, green walls and trees in urban green space.

As a form of vegetation, trees influence urban microclimate by controlling temperature at the pedestrian level and at the urban canyon level, thereby mitigating UHI impacts at the urban level. The effects of trees in urban areas are based on different scales, such as a tree at the building level, a row of trees in an urban canyon, a cluster of trees in parks and open spaces, and a forest. Trees influence urban microclimate through shading, photosynthesis and evapotranspiration. In tropical climates, temperatures under trees are relatively lower than those in open spaces. In field measurements conducted in Australia, trees in urban parks lowered temperatures by 2-2.5°C (Besir, A, 2018).

VGS (Vertical Greening System) or vertical garden refers to the growth of plants on the building envelope or support structure. Incorporating vegetation into building construction by adding greenery to the facade of a building is becoming increasingly popular. It is considered a building material because it contributes to the sustainability of the building in addition to providing significant ecological and environmental benefits. A study comparing the performance of VGS in four different climatic conditions found that the cooling and energy benefits of VGS are weather dependent. Depending on the building system, the supporting structure, and the type of plant and substrate used, VGS are divided into two main types: green facades and LW (living walls). Green facades are further divided into traditional or direct green facades, double-skinned green facades, and perimeter planters, and LWs are divided into panels, modules, or blankets. Many researchers are studying the benefits and characteristics of VGS in different climates. VGS in tropical climates are mainly used for passive cooling, energy efficiency and thermal comfort. The design of VGS should consider the characteristics, components, foliage, air chamber thickness and local climate for better performance and environmental sustainability. In areas with high population, land shortage and high land costs, greening systems for building envelopes can provide adequate greening (Besir, A, 2018).

GR (greenroof) is vegetation planted on the flat or pitched roofs of buildings. GR can be divided into extensive GR with smaller plants and thin substrate layers and intensive GR with thick substrate and larger plants. One of the main contributions of genetic resources in the urban environment is the reduction of heat and energy savings in urban buildings and the mitigation of UHI effects. Other benefits of GRs are stormwater management, aesthetic appeal, increased productivity, improved habitat, noise reduction, and pollution reduction. GRs control the thermal performance of buildings through shading, evaporative cooling, and the insulating properties of plants and growing media. Roof gardens mitigate UHI in tropical climates. rooftop gardens in Sri Lanka have reduced temperatures by 10-15°C. After installing a large GR on the roof of a building in Singapore, field measurements showed a reduction in surface temperature of up to 18°C. The thin substrate layer of rough GR, the dark substrate, and the low-lying vegetation of rough GR resulted in lower thermal performance than intensive GR systems. On the other hand, the extensive GR thin layer quickly released trapped heat and provided better cooling at night. The extensive system blocked about 60% of the heat gain (Besir, A, 2018).

1.2.2 Computational fluid dynamics model

In recent years, Computational Fluid Dynamics (CFD) has been introduced into the field of urban thermal and wind environment simulation with the development of computer science (Bo-ot et al., 2012, Declet-Barreto et al., 2016, Skelhorn et al., 2014). The principle of this method is to partition the study space into tiny finite elements. Within and between the elements, the calculations follow the basic fluid and thermal dynamics. Through iterative calculations, the details of the thermal environment can be simulated. The method becomes important because of its labor-saving and high-detail advantages. A typical application of the method is to predict and verify the impact on the building microclimate. In the academic field, the method is an important tool to validate the proposed theory. Its current application in urban planning is just beginning. One example is that with the help of CFD, Zhou et al. (2011) explore the green space planning of Liaoyang city and propose a strategy for future planning.

Modeling has been widely used by researchers to study microclimates at different scales and in different regions. Modeling is used to simulate the performance of different types of mitigation measures. A wider range of scenarios, technologies, and climate benefits need to be examined at various scales. The use of numerical simulations in microclimate studies is now increasing due to the increased capacity of computational resources. Vegetation has become the most complex element in numerical microclimate analysis due to its multifaceted interactions with radiation flow and evapotranspiration. However, most software does not consider the complexity of vegetation, such as roof vegetation types and wall vegetation, when simulating microclimates. Envi-met is considered as a holistic microclimate model that combines many urban complexities such as different species of vegetation, building materials and roads. In addition, Envi-met is the most accepted and validated software for simulating urban outdoor microclimates.

Based on the fundamental laws of hydrodynamics and thermodynamics, Envi-met can simulate the diurnal cycle of major climate variables, including air and soil temperature and humidity, wind speed and direction, and radiation fluxes, with typical horizontal resolutions of 0.5 to 5 m and time steps of 1 to 5 s. (Bruse & Fleer, 1998a; Envi-met, 2018; Huttner, 2012). The simulation requires two main input files: the area input file, which defines the building layout, vegetation, soil type, receptors (i.e., specific grids in the Envi-met model), and project location parameters, and the configuration file, which contains the simulation settings for initialized values of meteorological parameters, output folder names, and time definitions.

1.2.3 Multi-objective spatial optimization model

For optimal arrangement problems, using an optimal model to solve the problem is usually a good choice. Single-objective optimization problems, there is usually only one optimal solution, and the optimal solution can be obtained by relatively simple and commonly used mathematical methods. In a multi-objective optimization problem, each objective restricts each other, and the performance of one objective is often improved at the cost of losing the performance of other objectives. It is impossible to have a solution that optimizes the performance of all objectives (which means There may be a large negative correlation between these two goals).

The multi-objective optimization model is an algorithm model that can find the best solution or a set of solutions in multiple conflicting problems. In real problems, many goals have conflicting relationships, such as minimizing costs, maximizing benefits, and maximizing reliability. The multi-objective optimization model can find the optimal solution in such problems (Konak, Abdullah, 2006; Ehrgott, Matthias, 2014). In the past, multi-objective optimization models were mostly used in energy optimization, logistics problems (Xu, Liangfei, 2015; Sheu, Jiuh-Biing, 2007). However, recent studies have shown that multi-objective optimization models have been widely used in the optimization of UGS layout (Charity Nyelele, 2021; Wang, Qingfen, 2020).

There are many types of multi-objective optimization algorithms.

Genetic Algorithm (GA) is developed under the inspiration of the theory of biogeochemistry and genetics. Among them, the most important concepts in the theory of biochemical evolution and genetics are involved: gene recombination, gene mutation, and chromosome variation. GA uses a computer to simulate biological evolution. Through continuous iterations, the offspring that adapt to the environment will continue to multiply, and those that do not adapt to the environment will be eliminated, so as to gradually find the optimal solution.

NSGA-II is a variant of genetic algorithm. It introduces the concepts of fast non-dominant sorting, crowding degree, and elite strategy to reduce the complexity of non-inferior sorting genetic algorithm. It has the advantages of fast running speed and good solution set convergence. NSGA-II algorithm and other optimization algorithms have better convergence speed and effect in low-dimensional multi-objective operations. Since the objective functions considered in this study are the heat reduction benefit of UGS and the cost of UGS, the NSGA-II algorithm is selected.

Chapter 2. Method

2.1 Framework of the modeling and simulation

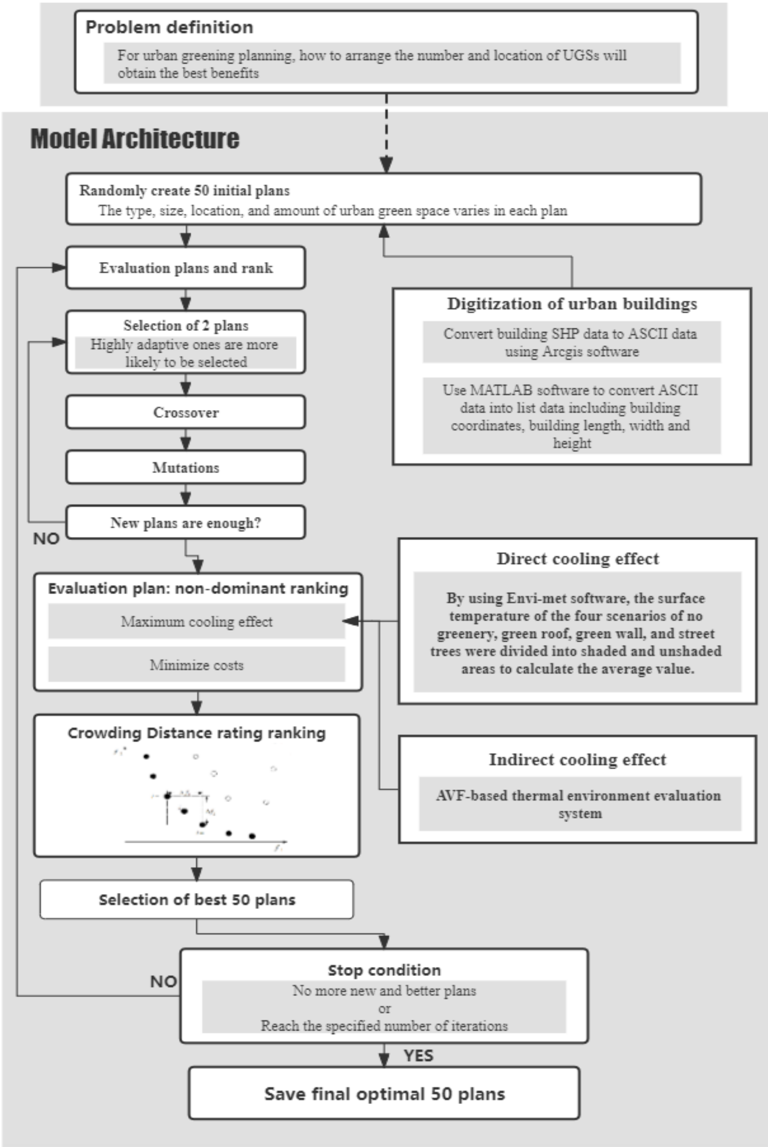

Figure 1 Spatial optimization for reducing UHI on 3D urban area

Our model employs an optimization approach that combines greening benefits (i.e., heat-reduction benefits from greening) and costs to determine where new green spaces should be built. The types of greening are roof greening, wall greening and trees. The main body of the optimization algorithm used is NSGA-II. The result data of Envi-met is processed and used as the input data of optimization algorithm for operation.

The construction of the 3D Multi-objective Optimization Model is shown in Figure 1. Firstly, 50 different layout schemes need to be created in a random way, each with different types of UGS, setting area, and setting position. The set of such schemes is called parent. Then new layout schemes are created by partially swapping and partially innovating the layout schemes of the parents through the selection, crossover, mutation part. The process is cycled 50 times. These newly generated layout solutions are the children.

The layout solutions of the parents and children are sorted non-dominantly by calculating the heat reduction effect, cost and congestion. The best 50 plans are eliminated by sorting and the remaining ones are eliminated, and the remaining plans are used as parents in a new round to continue the cycle. The cycle will end when no better plan is generated or when the set number of cycles is reached.

In order to allow the computer to randomize the layout of the UGS, the city's buildings need to be data. In the evaluation part of the heat reduction effect is divided into direct and indirect heat reduction effect. The calculation of the direct heat reduction effect is estimated by using Envi-met simulation data. Indirect heat reduction is estimated by means of radiation simulation. The cost is calculated by setting the type of UGS, the area and the type of plants.

2.2 Urban digitalization

The shp data of urban buildings, roads, and sidewalks are available on the Korean Land Information Platform website (http://map.ngii.go.kr). Since both Envi-met and 3D optimization models can only support the analysis of rectangular buildings, it is necessary to simplify the buildings from irregular shapes to rectangular shapes. The simplification was performed by Arcgis 10.8 software and the shp data were converted to ascii files. The ascii file was converted to a (X, Y, L, W, H) structure of the building using Matlab. Where X, Y are the point coordinates of the building, L, W, H are the length, width and height of the building. And then add the area proportion of green roof and the height of green wall after the building data (the order of green wall is East, West, North, South), such as (X, Y, L, W, H, RG, WGE, WGW, WGN, WGS) (Fig 2). The percentage of roof greening is set up in 6 levels from 0% to 100%. And the height of wall greening is set 6 levels from 0m to 30m. The location of street trees is determined by (TX, TY) coordinates. The distance of street trees from the road and the spacing between each other are determined according to the law of street trees in Korea. The random layout of greenery in the part of the model was determined by randomly generating variables for roof greenery, wall greenery and street tree layout.

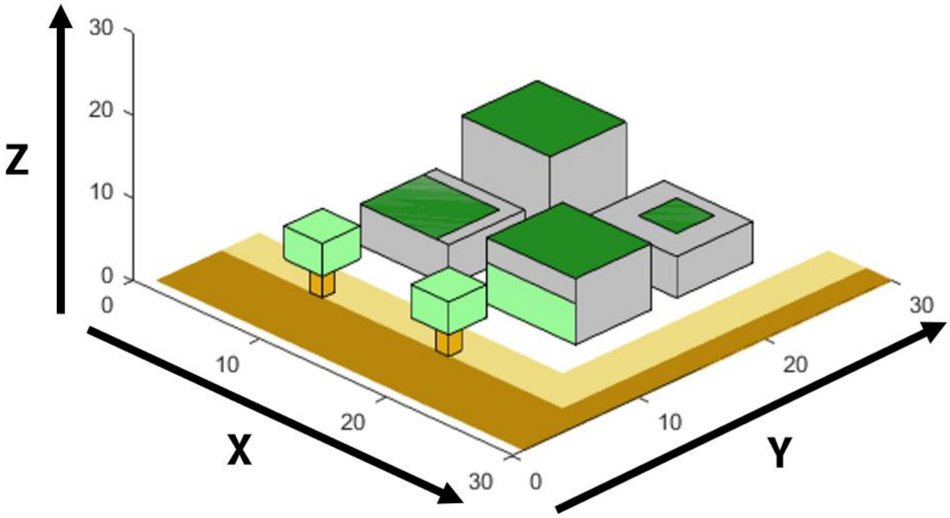

Figure 2 Visualization of buildings and greenery

2.3 Evaluation of cooling effect

Most researchers use CFD models to evaluate the thermal abatement benefits of greening facilities in three-dimensional space. However, due to the huge amount of calculation of the CFD model, a case analysis may last for several days, which is obviously not suitable for optimization models (Tsoka, S et al., 2018; Balany, Fatma et al.,2020). This study will develop a simplified thermal calculation method in combination with the CFD model, reducing the analysis time of a case to less than 1 second.

Bringing greenery to the surface of buildings is considered a technique to reduce building temperatures to 20 °C and also to reduce air conditioning energy consumption by 25 to 80%. For example, green roofs reflect 27% of the solar radiation, absorb 60% of it through photosynthesis, and transfer the remaining 13% to the growing medium.

The amount of change in surface temperature is an important evaluation tool when evaluating the effects of greenery in these areas. In addition, urban roads and surfaces occupy a large part of the urban space, and it is estimated that about 29-45% of the urban surface consists of pavement. Typically, in summer, pavement temperatures can be up to 20 °C higher than the surrounding environment, and the high absorption of heat by the pavement surface significantly contributes to the UHI effect. Therefore, surface temperature is also a very important part when evaluating the mitigation effect of greenery on UHI. Based on these bases, the amount of surface temperature change is used as an indicator to evaluate the cooling effect of greenery in this study.

In this study, the heat-reduction benefits of greening facilities are divided into two categories: direct heat-reduction benefits and indirect heat-reduction benefits. The direct heat reduction benefit is the heat reduction benefit value of the current location after the greening facility is implemented. It represents the surface temperature change of the wall or ground behind the current greening after the implementation of greening facilities.

The calculation of this value will be extrapolated in conjunction with the Envi-met software. We will use Envi-met to simulate the four cases without any greening, greening on all roofs, greening on all walls, and greening on trees. By calculating the average surface temperature of the wall or road behind green roofs, green walls, trees in shaded and non-shaded areas. And the difference between the surface temperature T_{before} without greening at this position and the set surface temperature value T_{after} is the direct cooling benefit Eq1.

$$Effect_{direct} = T_{before} - T_{after} \tag{1}$$

Table 1 Variables that need to be obtained by simulation in Envi-met

Symbol	Content	Average (yes/no)
T_{ws}	Ungreen wall surface temperature in shaded areas	No
T_w	Ungreen wall surface temperature in non-shaded areas	No
T_{ls}	Ungreen land surface temperature in shaded areas	No
T_l	Ungreen land surface temperature in non-shaded areas	No
RT_{ws}	Wall surface temperature of green roof in shaded area	Yes
RT_w	Wall surface temperature of green roofs in non-shaded areas	Yes
WT_{ws}	Wall surface temperature of wall greening in shaded area	Yes
WT_w	Wall surface temperature of wall greening in non-shaded areas	Yes
TT_{ls}	Surface temperature of tree greening in shaded areas	Yes
TT_l	Surface temperature of tree greening in non-shaded areas	Yes

The indirect cooling benefit refers to the cooling benefit caused by setting up greenery in other locations. It has been shown in several studies that heat conduction and heat convection account for a very small proportion of heat exchange generated by greening(Feng et al., 2010; He et al., 2016), so in this study only the benefits of heat radiation will be studied, without considering the effects of heat conduction and heat convection. And this study assumes that this point is not affected by the change of short-wave radiation caused by greening, and only considers the change of long-wave radiation caused by the reduction of surface temperature by greening.

In order to explore the surface temperature change induced by long-wave radiation, the received long-wave radiation change at each point is required, which is given by Eq2

$$\Delta LW = \sum_{i=1}^{n} \in * \partial (T_{before}^4 - T_{after}^4) * AVF_i \tag{2}$$

where T_{before} is the surface temperature before the greening of the long-wave radiation point, T_{after} is the surface temperature after greening, $\in$ is the thermal emissivity of the point, ∂ is the Stefan-Boltzmann constant, 5.67 X 10-8 W m- 2 K-4. AVF is the average view factor. n means that the affected point is affected by n points.

The surface temperature T_s can be derived from the surface energy balance equation Eq3. T_a is air temperature, v_{wind} is wind speed, B_0 is Bowen ratio, Q_s is storage heat flux, and Q is net radiation flux. The derivation of Q_s will use Eq4. The B_0 is set to 20, assuming that there is little latent heat in roofs, walls and floors.

$$T_s = T_a + \frac{Q - Q_s}{(6.2 + 4.26v_{wind})(1 + \frac{1}{B_0})} \tag{3}$$

$$Q_s = 0.51 \times Q - 34 \tag{4}$$

Using Eq3 and Eq4, the net radiation of the affected point can be calculated, and since the short-wave radiation is assumed to be unchanged, the change of the long-wave radiation is the net radiation change. Re-introduce Eq3 and Eq4 through the new net radiation change, to obtain the surface temperature after the point is affected by greening.

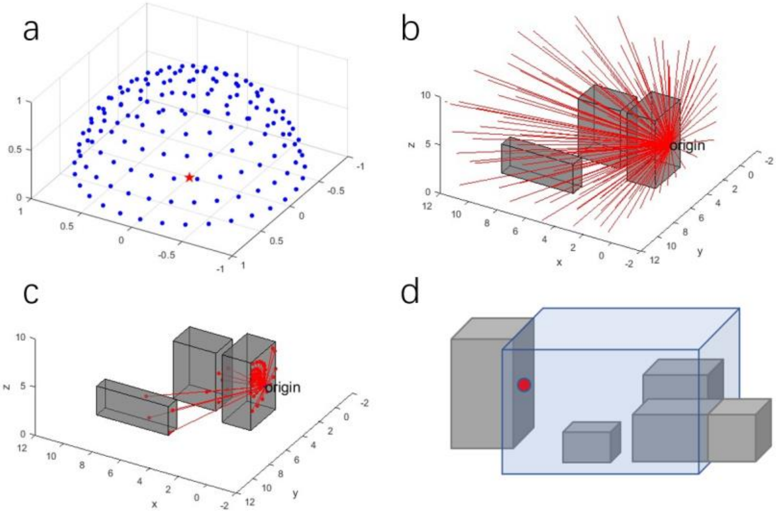

Figure 3 The calculation process of Average View Factor (AVF)

The calculation of Average View Factor (AVF) allows us to determine the magnitude of the impact of greening on the surrounding locations. For example, when the same greening is set up, the radiation impact on distant objects will be smaller. First, take the affected point as the origin, and divide the hemisphere at equal angles, as shown in Figure 3a. Connect the origin to the points on the semicircle to simulate rays, as shown in Figure 3b. By calculating the intersection of the ray with the first intersecting building face, as shown in Figure 3c. The grid represented by this intersection has an AVF of 1 / total number of rays for the affected points.

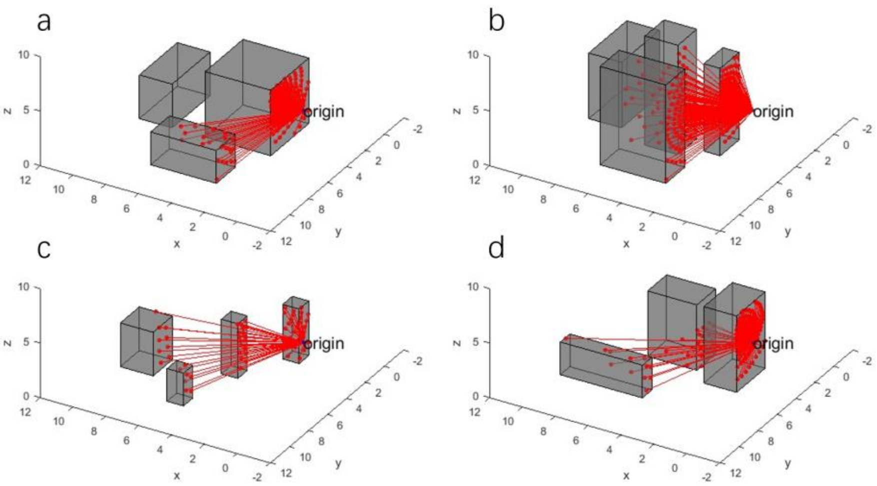

Figure 4 Ray tracing test

Theoretically, the more the number of rays, the more accurate the result will be, but the unlimited increase of rays will greatly increase the calculation amount of the model, so it is necessary to determine a reasonable number of rays. 4 different construction buildings were tested to determine the number of rays (Fig 4). The analysis is carried out by the AVF value of the building population and the value of the number of rays. In the same way, in order to constrain the calculation time as much as possible, a box is set up with the affected point as the center, and only the area inside the box is calculated. According to the results of multiple simulations of Envi-met, when the impact point and the affected point exceed 10m, the impact value can be ignored. Therefore, in this study, the vertical distance between the center of the box and each surface is set to 10m.

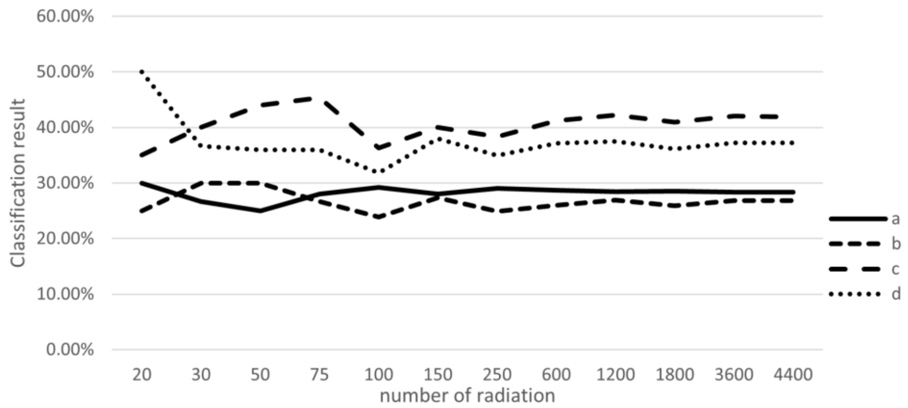

Figure 5 Classification result of Ray tracing test on different number of radiations

After a, b, c, d four cases of testing. It is found that the building AVF varies greatly when the number of rays is low (Fig.5). This is because when the number of rays is low, the spacing between rays is too large, resulting in errors. However, as the number of rays increases, this spacing will become smaller and smaller to reduce the generation of errors. This error will be reduced to an acceptable range when the number of rays is 600. And as the number of rays increases again, the results will change too much, but it will cause a large increase in the amount of model calculation. So, 600 seems like a reasonable value.

2.4 Cooling efficiency maximum

The size of roof greening is divided into 6 grades according to the percentage of roof area, and the same size of wall greening is divided into 6 grades in units of 5m. The maximum number of trees can be set to 11 according to regulations.

The cooling effect of the kth scheme $Effect_k$ is calculated according to the type, location and area of greening. Surface temperature calculations within a single mesh are as described above. The difference between the surface temperature in the grid without greening and the surface temperature in the grid after greening is used as the cooling benefit of the ith grid Eq5. I is the number of overall surface grids

$$Effect_i = T_{before\_i} - T_{after\_i} \tag{5}$$

$$Effect_k = \sum_{i=i}^{I} Effect_i \tag{6}$$

2.5 Cost minimization

If there are no cost constraints, the best strategy is to install vegetation whenever possible. However, the actual greening plan is created and executed within a certain budget. Changes in greening benefits must be visualized based on cost changes to support relevant decisions.

The cost of the kth plan can be calculated according to the type and size of the green space. In the previous study, the installation cost of green roofs ranged from 104$/m^2 to 306$/m^2 depending on the type and country, and the maintenance cost ranged from 10$/m^2/year to 32$/m^2/year(Niu, H., 2010; Bianchini, F., 2012; Peri, G., 2012). The installation and maintenance costs for green roofs were set at 135$/m^2 and 15$ respectively, taking into account the current situation of green roofs in Korea and the labor cost, since the buildings in the study area are short and simple in structure and therefore suitable for extensive green roofs. The installation cost of wall greening is in the range of 3-315$/m^2. Green façades require less material and are less expensive. Living walls, on the other hand, have a large price difference depending on the system. The maintenance cost of green walls ranges from 3-27$/m^2/year(Bianchini, F., 2012). The installation cost is set to 140$/m^2 and the maintenance cost is set to 10$/m^2/year in the context of the current situation in the study area. For the installation of street trees, there are corresponding planting strategies and regulations in Korea. Therefore, the most commonly used street tree is the Ginkgo tree with a height of 16m and a crown radius of 2.5m. The installation cost is 480$/tree and the maintenance cost is 30$/tree/year.

$$Cost_k = f(type, size) \tag{7}$$

2.6 Parameter setting for spatial optimization

The population number was set to 50, and the number of cycles was set to 10,000. After testing, within the study area, applying this setting was sufficient to obtain optimal results. The ratios of crossover and mutation are set to 0.3 and 0.2, respectively. This setting can fully improve the convergence speed and ensure the diversity of the population. The crossover is to exchange all the greening layout plans in the random space, and the mutation is to rearrange the greening in the random space in the current plan.

2.7 Application of the model

2.7.1 Simple urban block

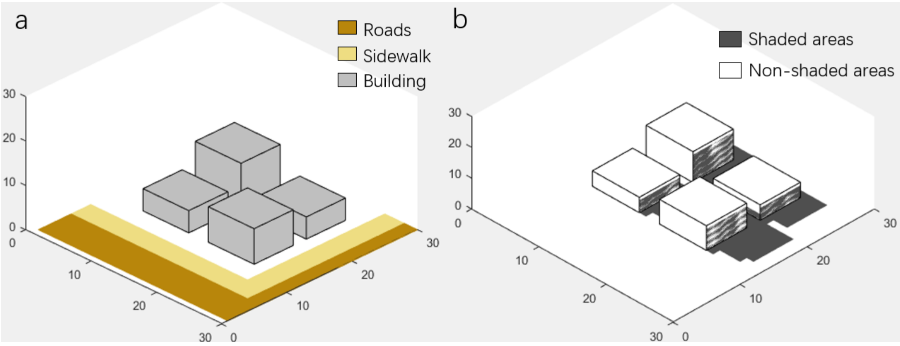

Figure 6 Distribution of building roads and shaded areas in a simple urban block

The 3D optimization model provides the most effective cooling benefits by selecting the most favorable locations. The 3D optimization model is applied using a hypothetical simple urban neighborhood to draw general conclusions about the relevance of the variables used. We use a simple city block at one of the corners of the intersection. The block has a dimension of 30m*30m and contains four buildings with heights of 5m, 8m, 10m, and 5m, as shown in Figure 6a. The shading of the buildings is shown in Figure 6b.

Sedum is used as a green roof plant in this simple urban block. sedum is widely used for green roofs because it is easy to manage, low cost, and can grow without thick substrate (Muhammad Shafique, 2018). Hedera helix will be chosen for the green plants on the walls. Hedera helix is a climbing plant, which is relatively adaptable to various climate types and Hedera helix is a climbing plant, which is relatively adaptable to various climate types and does not require high irrigation, so it is low cost to set up and easy to maintain. And because the leaves of the plant are relatively lush, it can provide sufficient shading effect for the building wall, and is widely used in wall greening all over the world (F Ascione, 2020). The street tree species selected is the most used street tree species in Korea, Ginkgo.

The temperature and humidity data are from the Korea Meteorological Agency Weather Data Open Portal. Statistics for the year 2021 show that the highest temperature date was July 24, with a maximum temperature of 37°C and a minimum temperature of 26.9°C. And the highest humidity is 75% and the lowest humidity is 45%. In order to effectively mitigate the temperature in the city, the hottest time of the day, 3 pm, was chosen as the analysis period.

2.7.2 Application to real city scenarios

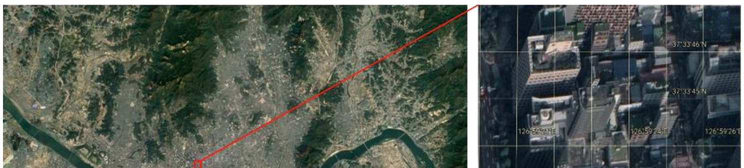

Figure 7 Study site

To reflect the applicability of the model to a real city scenario, a commercial district in Jung-gu, Seoul, South Korea was selected for simulation. The coordinates of this area are 126°59'24''E, 37°33'45''N. Britta Jnicke et al. (2019) analysis data shows that the Jung-gu region has the highest thermal vulnerability index. The buildings in this area vary in height and are densely constructed, which fully reflects the urban architectural characteristics of Seoul. There are enough walkways, roof areas, and wall areas in this area to arrange greenery.

As of December 2015, the total population is 125,733, and the total area is 10.0km2, which is 1.7% of the total area of 605.2 km2 in Seoul. In Jung-gu, Jangchung-dong occupies the largest area of 1.4 km2 and the smallest place is Donghwa-dong 0.3 km2. Jung-gu is a long topography from east to west, with high south and low north. Namsan 271m, one of the inner Sasan Mountains in Seoul, is located in the south, and Cheong-gye river through Jongro-gu to the north. It is a flat area between Namsan Mountains and Cheong-gye river and occupies the southern half of the Seoul Basin.

The buildings and roads in the area are more complex than in the simple urban neighborhoods, and the distribution of buildings and shaded areas are shown in Figure 8a, b. The greenery and meteorological data used in the area are the same as in the simple urban block.

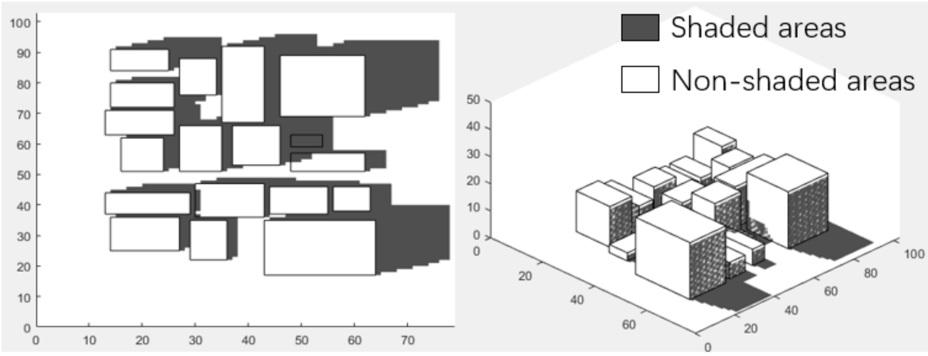

Figure 8 Distribution of buildings and shaded areas in the study area

Chapter 3. Result

3.1 Simple urban block

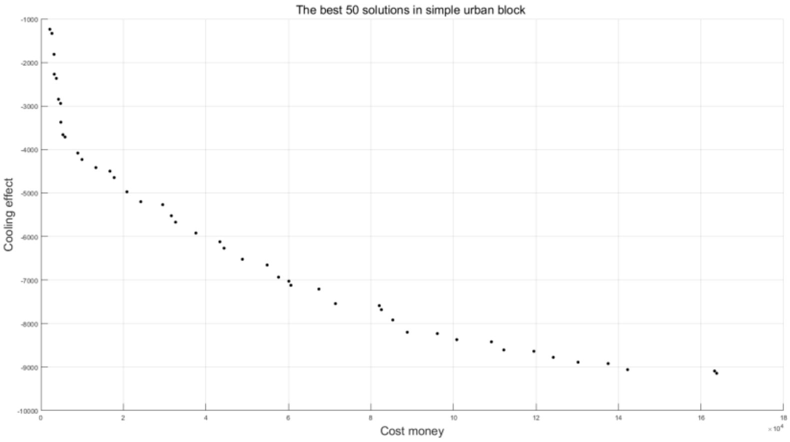

Figure 9 Pareto solution set for 3D optimization model

We applied the 3D optimization model to a hypothetical simple urban neighborhood to obtain the final 50 Pareto schemes (each black dot indicates an individual optimal scheme, Fig.9), showing the trade-off relationship between cooling effectiveness and cost by calculating the overall heat reduction benefits and greening construction costs for each scheme (Fig.9) An increase in the number and area of greenery will lead to an increase in the implementation cost, but also in the greening benefits. At lower costs, the greenery is mainly distributed in areas with higher cooling benefits (e.g., within non-shaded areas) or the type of greenery is mainly applied in types with higher benefits. And as the cost increases, the areas with lower cooling benefits are only selected, and the increase of heat reduction benefits gradually slows down. In order to find out which types of greenery or which locations of greenery imply better heat reduction benefits, the layouts of scenarios 2th, 4th, 11th, 16th, 30th, 50th were selected for detailed evaluation.

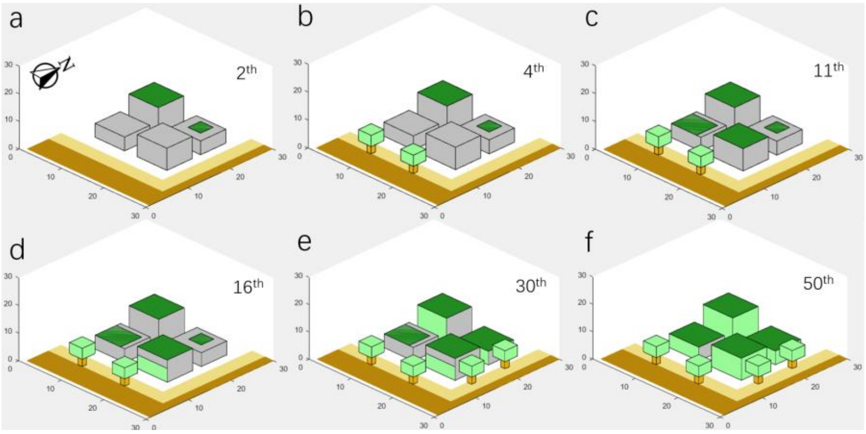

Figure 10 Specific greening layout schemes

the specific plans of the 2^{th}, 4^{th}, 11^{th}, 16^{th}, 30^{th}, and 50^{th} schemes. a, b, c, d, e, f with a viewpoint of 45°NW

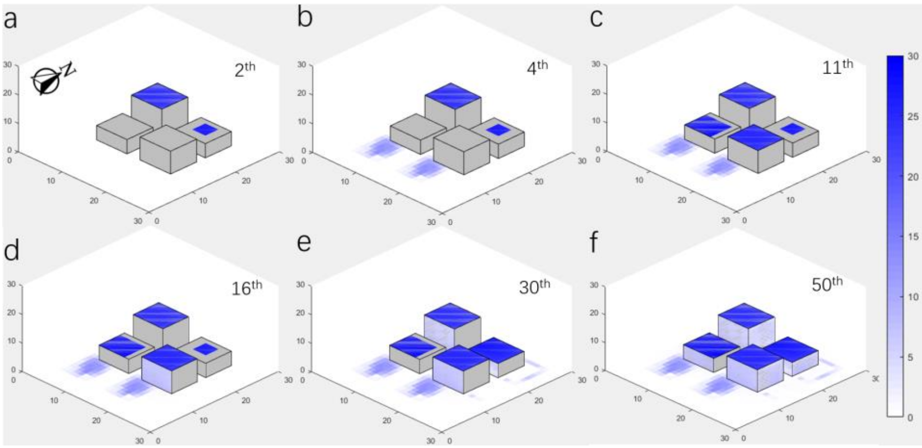

Figure 11 Cooling effect of specific schemes

the specific plans of the 2^{th}, 4^{th}, 11^{th}, 16^{th}, 30^{th}, and 50^{th} schemes. a,b,c,d,e,f with a viewpoint of 45°NW

Table 2 Total cooling effect and cost for each scenario

Objectives	2th	4th	11th	16th	30th	50th
Cooling effect (˚C)	1236	1812	3661	4498	6934	9144
Cost ($)	2,160	3,180	5,340	16,740	57,600	163,800

The layout plan of each scheme is shown in Figure 10, and the cooling effect is shown in Figure 11. The total cost of greening construction and the total surface temperature cooling of each scheme are shown in table 2. In Figure 10,11 a to f is the order of cost from less to more. As a whole, all greening types were not established in the shaded areas when the construction costs were insufficient or less. This is due to the fact that surfaces that are in shade receive much less solar radiation than other surfaces. The most important of the means of heat reduction from greenery is the blocking of solar radiation from reaching the surface of the building or the ground. Therefore, when the greenery is located in the shaded area, the heat reduction benefit is much lower than when it is located in the non-shaded area.

According to Figure 10a, b, c it can be seen that green roofs and street trees are arranged with higher priority than wall greening. And the priority of green roof and street trees are similar. This is due to the fact that the roof and the ground are horizontal, which itself receives more solar radiation than the walls. Therefore, when greenery causes blockage of solar radiation, it tends to block more of it out. And when green roofs are compared with street trees, each can be found to have its own advantages. Because green roofs are set up close to the ground level of the roof and provide the soil for plant growth, they can also provide a good radiation blocking effect. Therefore, green roofs provide more cooling effect when installed (Fig.11d). However, since green roofs only benefit the lower one square meter of the roof when set up, the cooling range of green roofs is relatively small. Street trees, on the other hand, because they possess a canopy, often create a shade to block radiation when one unit of street trees is set up. However, the canopy of a street tree is located farther from the ground than a green roof, and because there are voids within the canopy, radiation can pass through the canopy to the ground. Therefore, street trees can block less radiation than green roofs. Considered together, the cooling efficiency of rooftop greenery and street trees are relatively similar.

The cooling range of wall greening, like roof greening, only works on the wall behind the location where the wall greening is located, but because the wall is vertical, it receives less radiation intensity compared to the ground and roof, and therefore provides less benefit in blocking radiation than roof greening and street trees (Fig.11e). Therefore, depending on the cost from less to more, green roofs and street trees will be chosen first, followed by green walls. When comparing between wall greenery, it can be seen that wall greenery facing the sun will be established first than wall greenery not facing the sun. This is because walls that do not face the sun tend to be in the shade.

3.2 Evaluation of the evolutionary approach

In order to verify whether the 3D Multi-objective Optimization Model adequately reflects the effect of greening in the evaluation of heat reduction, a scheme was selected to construct the same greening layout in Envi-met for the calculation of surface temperature. The surface temperature data predicted by the model were compared with the surface temperature data in the Envi-met results. There are 1796 surfaces in a block of 30m*30m. The difference values of the surface temperature data predicted by the model and the surface temperature data in the Envi-met results were calculated. The difference values were counted using 1°C as a range (Fig.12)

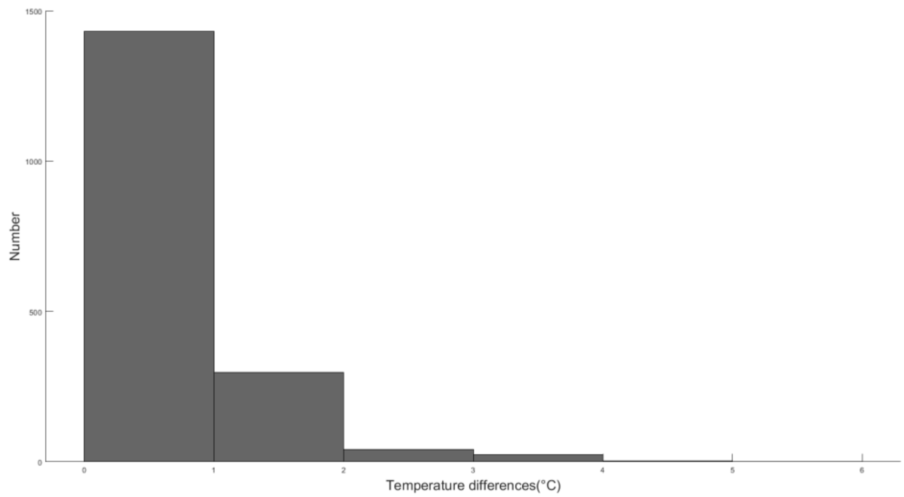

Figure 12 Statistics of the difference values between the surface temperature data predicted by the model and the surface temperature data from the Envi-met results

The comparison shows that the predicted results for most of the surfaces are equal and similar to the Envi-met results, but there are still some surfaces that differ from the Envi-met results by more than 1°C, and a small percentage of the surfaces have a difference value of

2°C or more. The reason for this discrepancy is because the model is run under some assumptions and simplifications when calculating the cooling benefits. For example, the surface temperature calculation for a green wall or green roof setup uses the average of Envi-met surface temperatures for all green setup locations in the non-shaded area when the wall is fully green or the roof is fully green. The effect on wall greening due to the formation of street trees is ignored. And only heat radiation is considered without calculating the effect of heat conduction and heat convection.

However, these assumptions and simplifications are inevitable, and if Envi-met is used to evaluate the cooling effect, at least 500,000 calculations are required in the optimization model. With a run time of about one hour on a medium to high end computer, it would take at least 57 years to perform the optimization calculations. The model was run in the experiment for about 10 hours, plus 4 hours for 4 simulations using Envi-met to construct the input data, for a total time of about 14 hours. Compared to the Envi-met model, the analysis time is greatly reduced making optimal analysis possible. The surface temperature data predicted by the model was compared with the surface temperature data from the Envi-met results and the R^2 and RMSE metrics were calculated (Fig.13) The R^2 result was 0.9949 and the RMSE result was 0.6198, which means that the resulting errors are within acceptable limits. And the surface present model already reflects the cooling effect triggered by greening to a large extent.

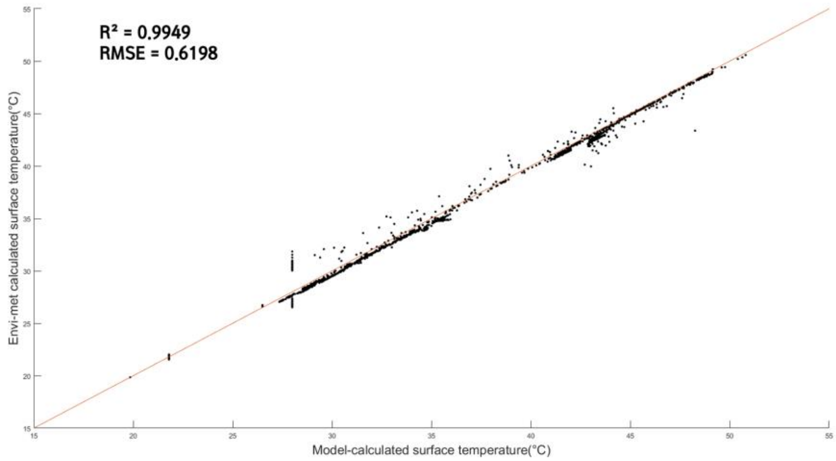

Figure 13 modelling validation using relationship between Envi-met simulation and proposed 3D spatial optimization

3.3 Real city scenarios

After completing the analysis of a simple urban block, the proposed methodology has been applied to a real case study of an urban green space to demonstrate its applicability. A set of 50 Pareto solutions on the greening layout of the study site was obtained by the model (Fig.14). In order to better analyze the layout within the real cases, the 3th, 8th, 16th, 20th, 34th and 45th scenarios have been selected for detailed analysis.

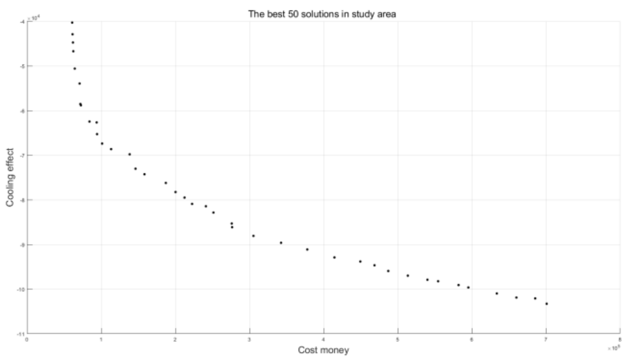

Figure 14 Pareto solution set in real city scenarios

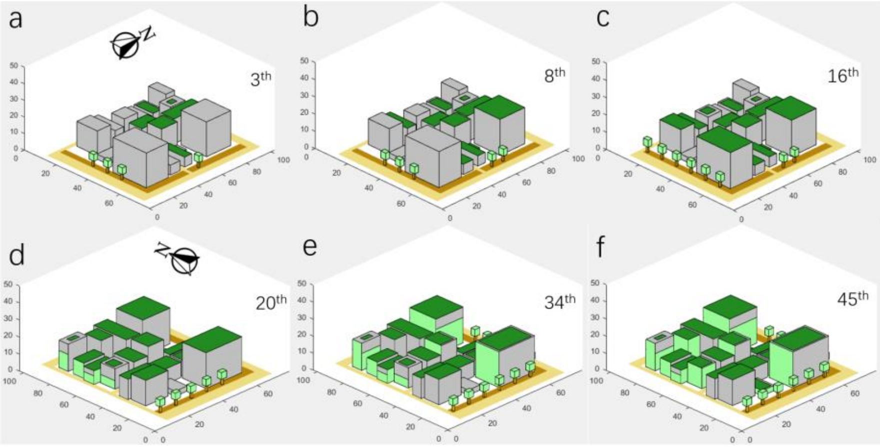

Figure 15 Individual greening arrangement scheme

represent the specific plans of the 3th, 8th, 16th, 20th, 34th, and 45th schemes. a,b,c with a viewpoint of 45°NW and d,e,f with a viewpoint of 45°NE

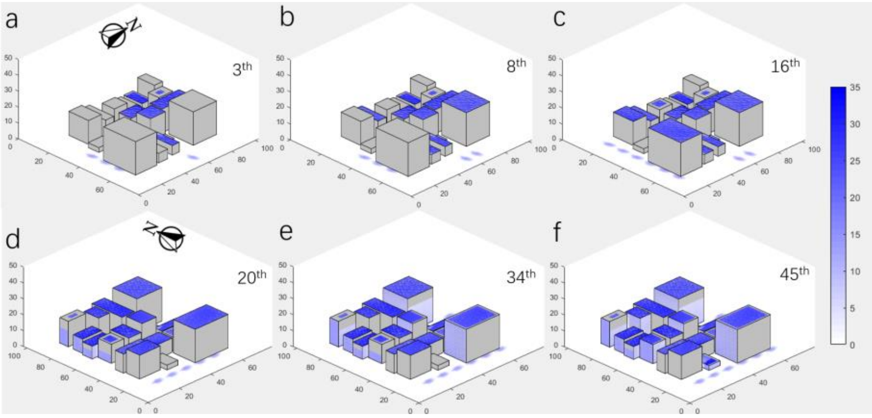

Figure 16 Individual greening cooling effects at the study site.

a,b,c,d,e,f represent the specific plans of the 3th, 8th, 16th, 20th, 34th, and 45th schemes. a,b,c with a viewpoint of 45°NW and d,e,f with a viewpoint of 45°NE

Table 3 Total cooling effect and cost for each scenario in study area

Objectives	3th	8th	16th	20th	34th	45th
Cooling effect (°C)	17963	30551	50995	59102	77054	85797
Cost ($)	19,920	32,670	61,440	119,070	409,230	646,590

Since the buildings in the study area are more complex, a 45° north-west view was used in a,b,c and a 45° north-east view was used in d,e,f to better show the layout of the greenery (Fig.15 16). With Fig. 15a,b,c we can see the same results as for the simple urban block, where the green roofs and street trees appear before the wall greenery. This indicates that the cooling efficiency of green roofs and street trees is higher than that of wall greening. In addition to this we find an interesting phenomenon, by comparing the three cases a,b,c, we can find that the green roofs of the lower buildings have a higher priority than the green roofs of the higher buildings. This is due to the fact that when green roofs are installed on lower buildings, they can reduce the surface temperature of the surrounding high-rise building walls by reducing the emission of long-wave radiation. In contrast, the roofs of high-rise buildings do not affect the surrounding buildings even if the long-wave radiation is lowered because there are no surrounding walls. Similarly multiple low wall greening has a higher priority than one high wall greening (Figure 15 d,e,f). By lowering the surface temperature, the low wall greening reduces the emitted long-wave radiation, which will affect the temperature of the ground surface or other building surfaces.

In summary, the most influential element for the layout of greenery is whether it is a shaded area or not. Arranging greenery in the shaded area will greatly reduce the cooling efficiency of greenery. Secondly, the type of greenery is an important factor that affects the cooling efficiency of greenery, and we found that roof greenery and street trees have better efficiency compared to wall greenery. Furthermore, the location of the greenery is also a factor that affects the cooling efficiency of greenery. Having more building surfaces or ground surfaces within the cooling radius of the greenery tends to provide higher cooling efficiency.

Chapter 4. Discussion

The data needed for the 3D multi-objective optimization model include building data, weather data, plant data, construction cost data and surface temperature data calculated by Envi-met. This also means that the model is suitable for the analysis of any urban block. However, due to its computational complexity and computer runtime limitations, it still requires more than 2 days of runtime when analyzing areas over 200m*200m. Although the model has been greatly simplified in calculating the cooling effect, it still requires a large number of operations to calculate the AVF or to calculate the amount of long-wave radiation change on each surface. These calculations are inevitable, and if this process is omitted, the error will be greatly enlarged. Therefore, the use of the model is limited when the study area is large. When analyzing a large area, the area can be divided into several blocks for separate analysis.

For this model, cost is one of the very important input data. Different cost data may give completely different results. In this study the mean value is used for the calculation. In practice, the input of detailed cost data will give a better fit with local policies or market conditions. Similarly, only individual plant combinations and greening methods are shown in this study, e.g. extensive rooftop greening with sedum planting. The appropriate plants and greening methods vary from region to region and from country to country or from policy to policy. The method can be specified in detail by adjusting the plant data and the thickness of the substrate of the green roof, which will have an impact on the final result.

In this study, the amount of change in surface temperature was used as an evaluation metric, where roofs, walls and pavements were given a weighting of 1. However, the points that planners wish to focus on may be different for different areas. For example, if thermal comfort for pedestrians is desired as a goal, the greening of roofs and walls can have a smaller effect, so the weight of pavement needs to be increased. Or if the planner wants to aim at reducing the energy consumption of the building, then the weights of roofs and walls should be increased.

Further analysis of the errors generated by the model is performed. The surface temperature data calculated by the model for scenario 16 in the simple urban block were subtracted from the surface temperature data calculated by Envi-met, and the distribution of the difference values is shown in Fig. 17. positive values indicate that the temperature data calculated by the model are larger than those calculated by Envi-met, and conversely negative values indicate that the temperature data calculated by the model are smaller than those calculated by Envi-met. The wall and the ground part except the tree shade are in the over-evaluation of the surface temperature. Although the model calculates the long-wave radiation change due to greening and thus the cooling effect on the surrounding environment, it does not consider the heat convection phenomenon caused by the reduction of air temperature due to greening generation. The model has an underestimation when calculating the surface temperature in the shaded part produced by the trees. This is due to the fact that the cooling effect of the street tree is derived from the cooling effect of one tree in the Envi-met analysis. However, as the location of the tree changes, the surrounding environment changes, which can lead to a different radiative environment around the tree, resulting in a different cooling effect for each tree, but the model assumes the same cooling effect for each corresponding grid in the shadows caused by the tree.

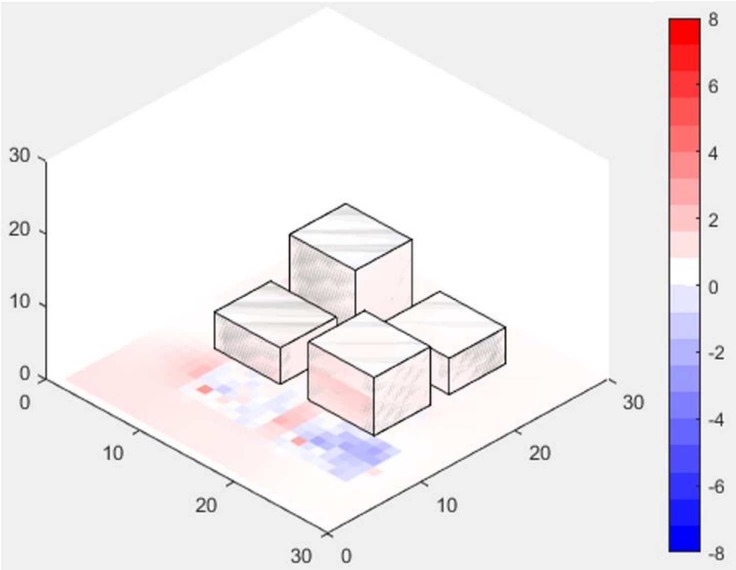

Figure 17 The difference between the surface temperature data calculated by the model and the surface temperature data calculated by Envi-met

For the results, we find that the cooling efficiency of green roofs and street trees is greater than that of green walls, but this does not mean that green walls are useless. In urban spaces, there are significant limitations to the establishment of street trees due to the regulations for their installation. As for buildings, the area of their roofs is much smaller than the area of their walls. Therefore, the installation of wall greenery is no less than the total amount of green roofs and street trees in terms of cooling. Taking a simple city block as an example, the total amount of heat reduction provided by wall greening is the largest when all greening is set up in the area where greening can be set up (Table 4), occupying 46.6% of the total heat reduction. In contrast, since street trees can only be set up four in the area and by two located in the shaded area, the total amount of heat reduction provided is the least, accounting for only 8.4% of the overall amount. Therefore wall greening is also an important part of urban greening construction.

Table 4 Variation of heat reduction provided by different types of greenery

Types of greenery	Wall greening	Roof greening	Street Trees
Total heat reduction (˚C)	4410	4259	789
Percentage of the total	46.6%	45%	8.4%

Chapter 5. Conclusion

The 3D Multi-objective Optimization Model optimizes the layout of green roofs, green walls and street trees based on two objective functions: maximizing the cooling benefits of greenery and minimizing the costs. The model is able to create a digital model of the city in 3D space and evaluate the indirect cooling effect of greenery by calculating the variation of long-wave radiation, and the direct cooling effect by using Envi-met data. Through the analysis of the results, the most influential element for the layout of greenery is whether it is a shaded area or not. Arranging greenery in the shaded area will greatly reduce the cooling efficiency of greenery. Secondly, the type of greenery is an important factor that affects the cooling efficiency of greenery, and we found that roof greenery and street trees have better efficiency compared to wall greenery. Furthermore, the location of the greenery is also a factor that affects the cooling efficiency of greenery. Having more building surfaces or ground surfaces within the cooling radius of the greenery tends to provide higher cooling efficiency.

Bibliography

Sun, A., Chen, T., Niu, R. Q., & Trinder, J. C. (2016). Land use/cover change and the urbanization process in the Wuhan area from 1991 to 2013 based on MESMA. Environmental Earth Sciences, 75(17), 1-12.

Debbage, N., & Shepherd, J. M. (2015). The urban heat island effect and city contiguity. Computers, Environment and Urban Systems, 54, 181-194.

Oliveira, S., Andrade, H., & Vaz, T. (2011). The cooling effect of green spaces as a contribution to the mitigation of urban heat: A case study in Lisbon. Building and environment, 46(11), 2186-2194.

Getter, K. L., & Rowe, D. B. (2006). The role of extensive green roofs in sustainable development. HortScience, 41(5), 1276-1285.

Ng, E., Chen, L., Wang, Y., & Yuan, C. (2012). A study on the cooling effects of greening in a high-density city: An experience from Hong Kong. Building and environment, 47, 256-271.

Bowler, D. E., Buyung-Ali, L., Knight, T. M., & Pullin, A. S. (2010). Urban greening to cool towns and cities: A systematic review of the empirical evidence. Landscape and urban planning, 97(3), 147-155.

Jing, C., Wenyong, T., & Bo, Y. (2011). The Structure of Urban Green Space System to tackle Heat-island Effect. Research Journal of Chemistry and Environment, 15(2), 755-758.

Liu, J., Zhang, L., Zhang, Q., Zhang, G., & Teng, J. (2021). Predicting the surface urban heat island intensity of future urban green space development using a multi-scenario simulation. Sustainable Cities and Society, 66, 102698.

Chow, W. T., Akbar, S. N. A. B. A., Heng, S. L., & Roth, M. (2016). Assessment of measured and perceived microclimates within a tropical urban forest. Urban Forestry & Urban Greening, 16, 62-75.

Dimoudi, A., & Nikolopoulou, M. (2003). Vegetation in the urban environment: microclimatic analysis and benefits. Energy and buildings, 35(1), 69-76.

Taha, H. (1997). Urban climates and heat islands: albedo, evapotranspiration, and anthropogenic heat. Energy and buildings, 25(2), 99-103.

Polo-Labarrios, M. A., Quezada-García, S., Sánchez-Mora, H., Escobedo-Izquierdo, M. A., & Espinosa-Paredes, G. (2020). Comparison of thermal performance between green roofs and conventional roofs. Case Studies in Thermal Engineering, 21, 100697.

Addo-Bankas, O., Zhao, Y., Vymazal, J., Yuan, Y., Fu, J., & Wei, T. (2021). Green walls: A form of constructed wetland in green buildings. Ecological Engineering, 169, 106321.

Bajsanski, I., Stojaković, V., & Milošević, D. (2019). Optimizing trees distances in urban streets for insolation mitigation. Geographica Pannonica, 23(4), 329-336.

Shah, A., Garg, A., & Mishra, V. (2021). Quantifying the local cooling effects of urban green spaces: Evidence from Bengaluru, India. Landscape and Urban Planning, 209, 104043.

Du, H., Cai, W., Xu, Y., Wang, Z., Wang, Y., & Cai, Y. (2017). Quantifying the cool island effects of urban green spaces using remote sensing Data. Urban Forestry & Urban Greening, 27, 24-31.

Zhang, Y., Murray, A. T., & Turner Ii, B. L. (2017). Optimizing green space locations to reduce daytime and nighttime urban heat island effects in Phoenix, Arizona. Landscape and Urban Planning, 165, 162-171.

Yoon, E. J., Kim, B., & Lee, D. K. (2019). Multi-objective planning model for urban greening based on optimization algorithms. Urban Forestry & Urban Greening, 40, 183-194.

Peng, S., Piao, S., Ciais, P., Friedlingstein, P., Ottle, C., Bréon, F. M., ... & Myneni, R. B. (2012). Surface urban heat island across 419 global big cities. Environmental science & technology, 46(2), 696-703.

Oke, T. R. (1988). The urban energy balance. Progress in Physical geography, 12(4), 471-508.

Jones, P. D., Lister, D. H., & Li, Q. (2008). Urbanization effects in large - scale temperature records, with an emphasis on China. Journal of Geophysical Research: Atmospheres, 113(D16).

Fujibe, F. (2009). Detection of urban warming in recent temperature trends in Japan. International Journal of Climatology: A Journal of the Royal Meteorological Society, 29(12), 1811-1822.

McCarthy, M. P., Best, M. J., & Betts, R. A. (2010). Climate change in cities due to global warming and urban effects. Geophysical research letters, 37(9).

Santamouris, M. (2014). On the energy impact of urban heat island and global warming on buildings. Energy and Buildings, 82, 100-113.

Tan, J., Zheng, Y., Tang, X., Guo, C., Li, L., Song, G., ... & Chen, H. (2010). The urban heat island and its impact on heat waves and human health in Shanghai. International journal of biometeorology, 54(1), 75-84.

Heng, S. L., & Chow, W. T. (2019). How 'hot'is too hot? Evaluating acceptable outdoor thermal comfort ranges in an equatorial urban park. International journal of biometeorology, 63(6), 801-816.

Blum, J. (2017). Contribution of ecosystem services to air quality and climate change mitigation policies: the case of urban forests in Barcelona, Spain. In Urban forests (pp. 21-54). Apple Academic Press.

Liu, F., Tian, Y., Jim, C., Wang, T., Luan, J., & Yan, M. (2021). Residents' Living Environments, Self-Rated Health Status and Perceptions of Urban Green Space Benefits. Forests, 13(1), 9.

Heng, S. L., & Chow, W. T. (2019). How 'hot'is too hot? Evaluating acceptable outdoor thermal comfort ranges in an equatorial urban park. International journal of biometeorology, 63(6), 801-816.

Besir, A. B., & Cuce, E. (2018). Green roofs and facades: A comprehensive review. Renewable and Sustainable Energy Reviews, 82, 915-939.

Zhou, Y., Shi, T., Hu, Y., Gao, C., Liu, M., Fu, S., & Wang, S. (2011). Urban green space planning based on computational fluid dynamics model and landscape ecology principle: A case study of Liaoyang City, Northeast China. Chinese geographical science, 21(4), 465-475.

Skelhorn, C., Lindley, S., & Levermore, G. (2014). The impact of vegetation types on air and surface temperatures in a temperate city: A fine scale assessment in Manchester, UK. Landscape and Urban Planning, 121, 129-140.

Declet-Barreto, J., Brazel, A. J., Martin, C. A., Chow, W. T., &

Harlan, S. L. (2013). Creating the park cool island in an inner-city neighborhood: heat mitigation strategy for Phoenix, AZ. Urban Ecosystems, 16(3), 617-635.

Bo-Ot, L. M., Wang, Y. H., Chiang, C. M., & Lai, C. M. (2012). Effects of a green space layout on the outdoor thermal environment at the neighborhood level. Energies, 5(10), 3723-3735.

Bruse, M., & Fleer, H. (1998). Simulating surface–plant–air interactions inside urban environments with a three dimensional numerical model. Environmental modelling & software, 13(3-4), 373-384.

Huttner, S. (2012). Further development and application of the 3D microclimate simulation ENVI-met (Doctoral dissertation, Mainz, Univ., Diss., 2012).

Xu, L., Mueller, C. D., Li, J., Ouyang, M., & Hu, Z. (2015). Multi-objective component sizing based on optimal energy management strategy of fuel cell electric vehicles. Applied energy, 157, 664-674.

Sheu, J. B. (2007). An emergency logistics distribution approach for quick response to urgent relief demand in disasters. Transportation Research Part E: Logistics and Transportation Review, 43(6), 687-709.

Konak, A., Coit, D. W., & Smith, A. E. (2006). Multi-objective optimization using genetic algorithms: A tutorial. Reliability engineering & system safety, 91(9), 992-1007.

Ehrgott, M., Ide, J., & Schöbel, A. (2014). Minmax robustness for multi-objective optimization problems. European Journal of Operational Research, 239(1), 17-31.

Wang, Q., & Zeng, X. (2020). Energy-saving optimisation method for green space planning of urban gardens based on artificial bee colony algorithm. International Journal of Global Energy Issues, 42(5-6), 393-408.

Tsoka, S., Tsikaloudaki, A., & Theodosiou, T. (2018). Analyzing the ENVI-met microclimate model's performance and assessing cool materials and urban vegetation applications–A review. Sustainable cities and society, 43, 55-76.

Balany, F., Ng, A. W., Muttil, N., Muthukumaran, S., & Wong, M. S. (2020). Green infrastructure as an urban heat island mitigation strategy—a review. Water, 12(12), 3577.

Jänicke, B., Holtmann, A., Kim, K. R., Kang, M., Fehrenbach, U., & Scherer, D. (2019). Quantification and evaluation of intra-urban heat-stress variability in Seoul, Korea. International journal of biometeorology, 63(1), 1-12.

Shafique, M., Kim, R., & Rafiq, M. (2018). Green roof benefits, opportunities and challenges–A review. Renewable and Sustainable Energy Reviews, 90, 757-773.

Ascione, F., De Masi, R. F., Mastellone, M., Ruggiero, S., & Vanoli, G. P. (2020). Green walls, a critical review: Knowledge gaps, design parameters, thermal performances and multi-criteria design approaches. Energies, 13(9), 2296.

Niu, H., Clark, C., Zhou, J., & Adriaens, P. (2010). Scaling of economic benefits from green roof implementation in Washington, DC. Environmental science & technology, 44(11), 4302-4308.

Bianchini, F., & Hewage, K. (2012). Probabilistic social cost-benefit analysis for green roofs: A lifecycle approach. Building and environment, 58, 152-162.

Peri, G., Traverso, M., Finkbeiner, M., & Rizzo, G. (2012). The cost of green roofs disposal in a life cycle perspective: Covering the gap. Energy, 48(1), 406-414.